Figures and figure supplements

Antagonistic role of the BTB-zinc finger transcription factors Chinmo and Broad-Complex in the juvenile/pupal transition and in growth control

Sílvia Chafino *et al.*

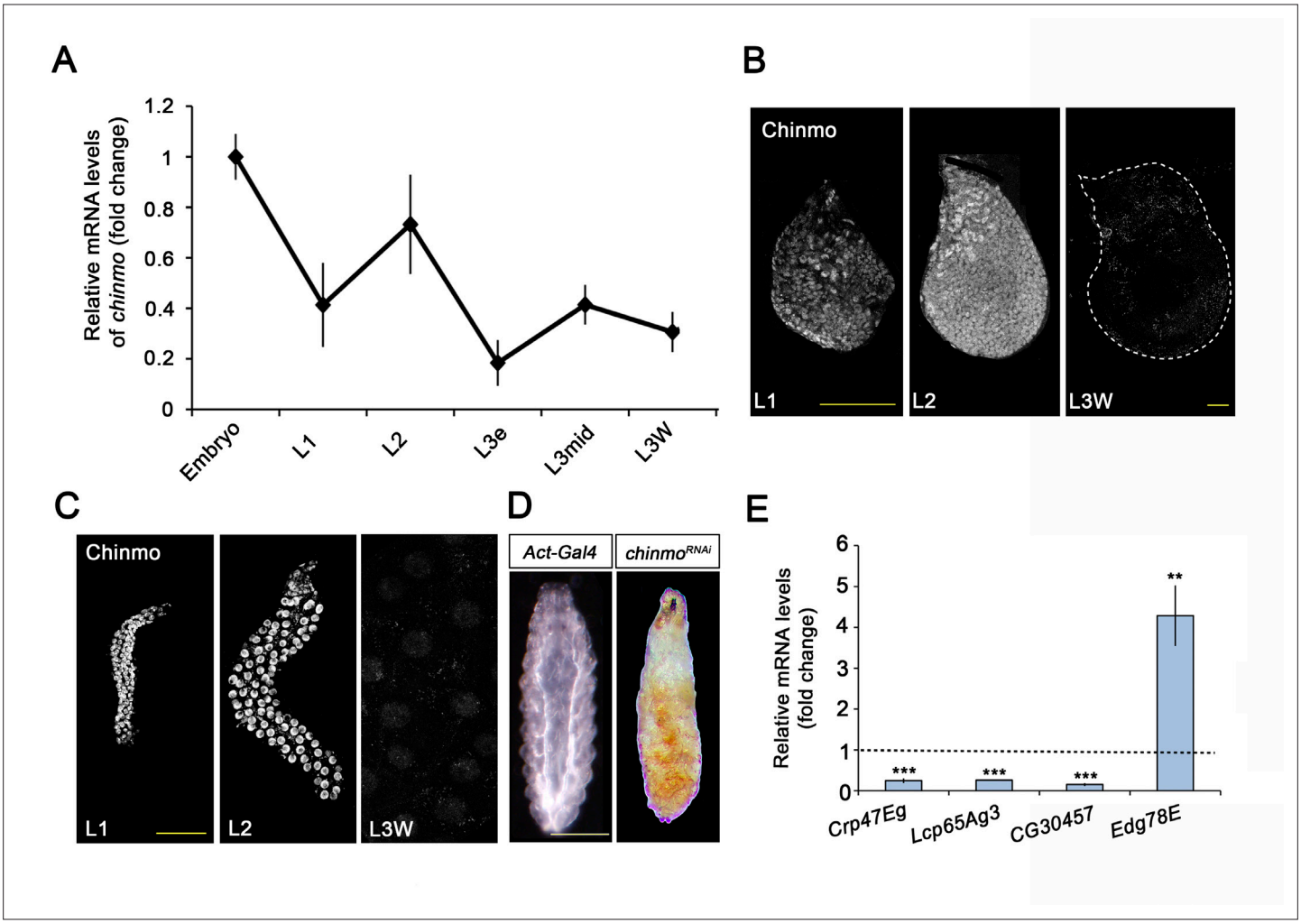

Figure 1. Chinmo is expressed during early larval stages and is essential for proper larval development. (**A**) *chinmo* mRNA levels measured by quantitative real-time reverse transcriptase polymerase chain reaction (qRT-PCR) from embryo to the wandering stage of L3 (L3W). Transcript abundance values were normalised against the *Rpl32* transcript. Fold changes were relative to the expression of embryo, arbitrarily set to 1. Error bars indicate the SEM (n = 3). (**B–C**) Chinmo protein levels in the wing disc (**B**) and salivary glands (**C**) of larval L1, L2, and L3W (females) stages. (**D**) Compared with the control (*Act-Gal4*), overexpression of *UAS chinmo*^{RNAi} in the whole body induced developmental arrest at the L1 stage. Scale bars represent 50 µm (**B and C**) and 0.5 mm (**D**). (**E**) Relative expression of larval-specific (*Crp47Eg, Lcp65Ag3, and CG30457*) and pupal-specific genes (Edg78E) in *UAS-chinmo*^{RNAi} L1 larvae measured by qRT-PCR. Transcript abundance values were normalised against the *Rpl32* transcript. Fold changes were relative to the expression in control larvae, arbitrarily set to 1 (dashed black line). Error bars indicate the SEM (n = 3). Statistical significance was calculated using t test (***p ≤ 0.001; **p ≤ 0.005).

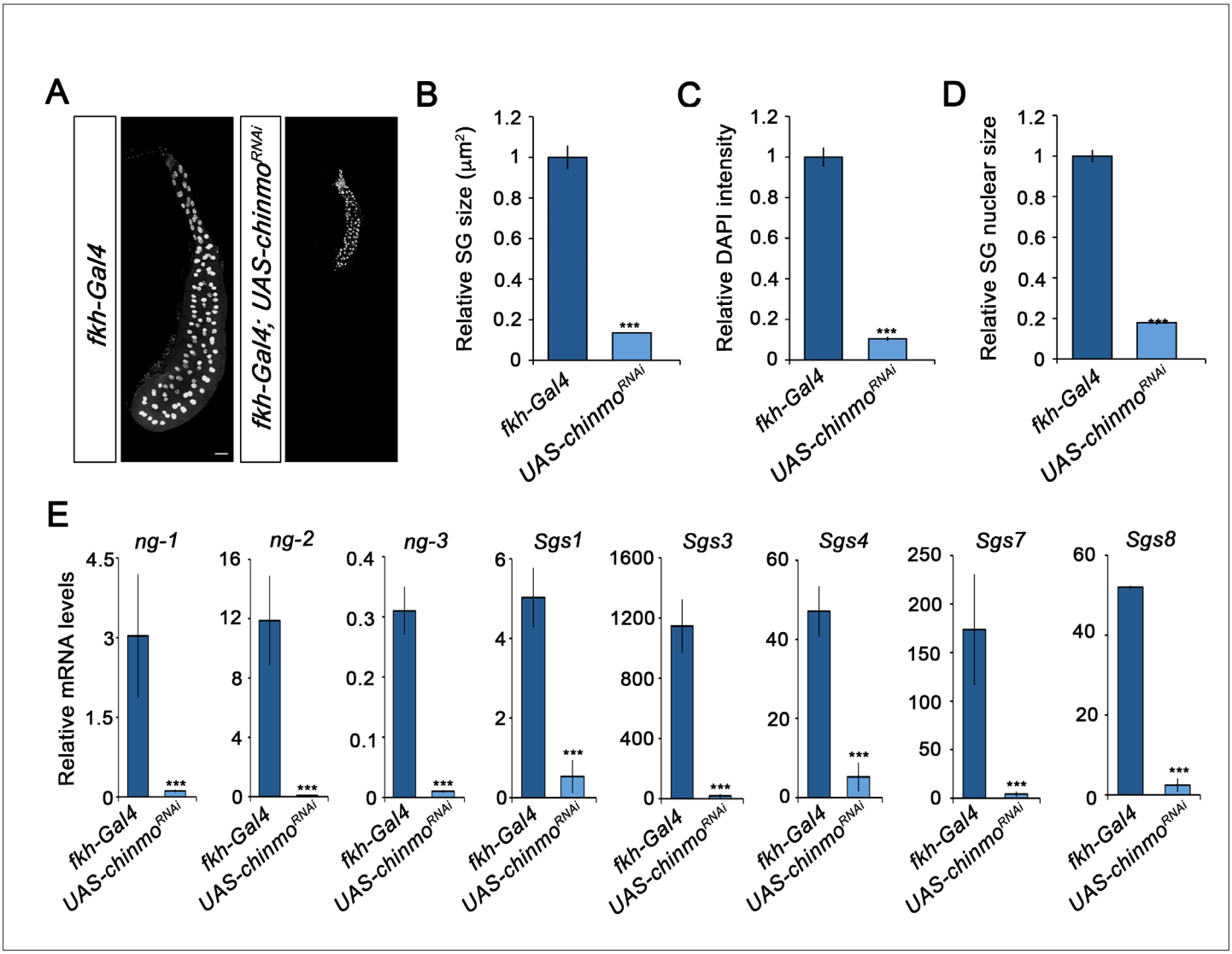

Figure 2. Chinmo is required for proper growth and function of the salivary glands during larval development. (**A**) DAPI staining of salivary glands from control (*fkh-Gal4*) and *UAS-chinmo*^{RNAi} larvae at L3W. Scale bar represents 50 µm. (**B–D**) Comparison of the relative size of salivary glands (n = 10 for each genotype) (**B**), DAPI intensity (n = 50 for each genotype) (**C**), and nucleic size of salivary glands (n = 50 for each genotype) (**D**) between *UAS-chinmo*^{RNAi} and control larvae at L3W. Error bars indicate the SEM (n = 5–8). (**E**) Relative expression of *ng1-3* and *Salivary glands secretion* genes (*Sgs*) in *UAS-chinmo*^{RNAi} L3W animals measured by quantitative real-time reverse transcriptase polymerase chain reaction (qRT-PCR). Transcript abundance values were normalised against the *Rpl32* transcript. Error bars indicate the SEM (n = 5–8). Statistical significance was calculated using t test (***p≤0.001).

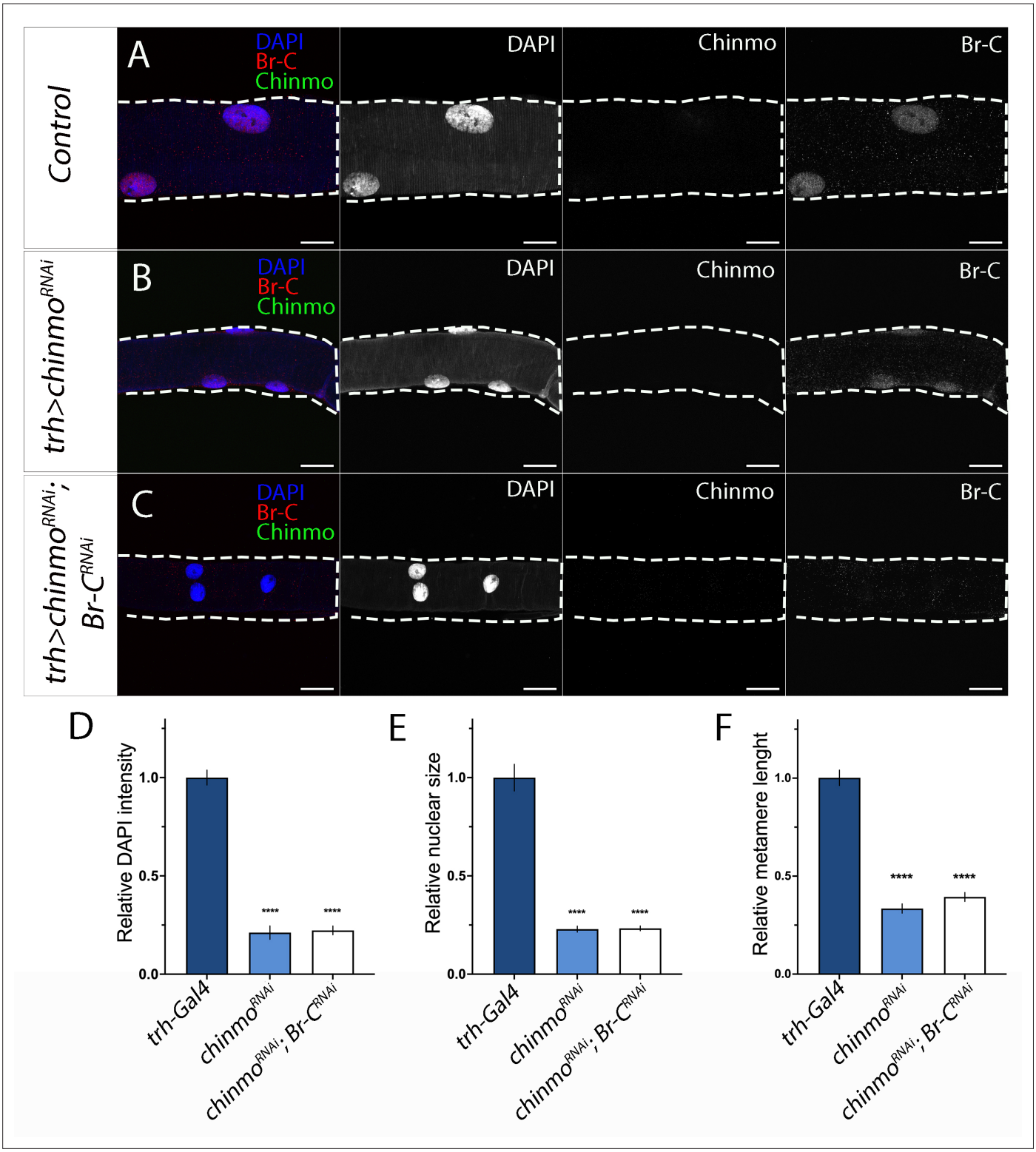

Figure 2—figure supplement 1. The role of *Chinmo* in the larval tracheal system. (**A–C**) Chinmo (in green), Br-C (in red) and DAPI-stained trachea from control (*trh-Gal4*) (**A**), *UAS-chinmo*^{RNAi} (**B**) and *UAS-Br-C*^{RNAi}*; UAS-chinmo*^{RNAi} (**C**) mid L3 larvae. Growth defect of tracheal cells induced by the absence of *chinmo* (**B**) was not rescued by Br-C depletion (**C**). (**D–F**) Comparison of the relative size of the trachea by measuring (n = 10 for each genotype) (**D**), DAPI intensity (**E**), and nucleic size of tracheal cells (**F**), and tracheal metamere length of control, *UAS-chinmo*^{RNAi} and *UAS-Br-C*^{RNAi}*; UAS-chinmo*^{RNAi} mid L3 larvae. Error bars indicates the SEM (n = 5–8). Statistical significance was calculated using t test (****p≤0.001). Scale bars represent 50µm.

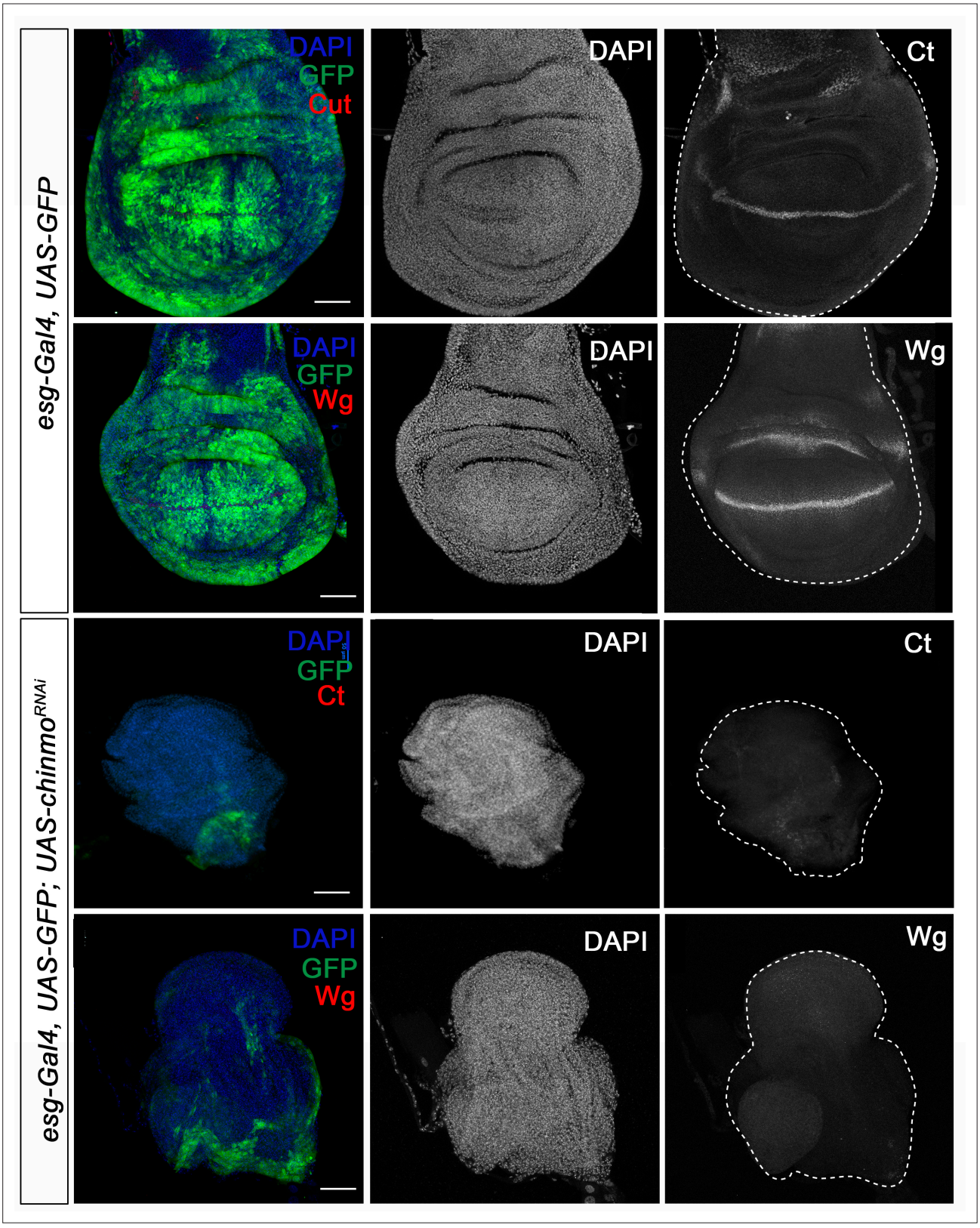

Figure 3. Chinmo is necessary for wing development during the larval period. Expression of Ct and Wg in wing discs of control (*esg-Gal4*) and *UAS-chinmo*^{RNAi} L3W larvae. Wing discs were labelled to visualise the *esg* domain (GFP in green) and nuclei (DAPI). Ct and Wg were not detected in *UAS-chinmo*^{RNAi}. Scale bars represent 50µm.

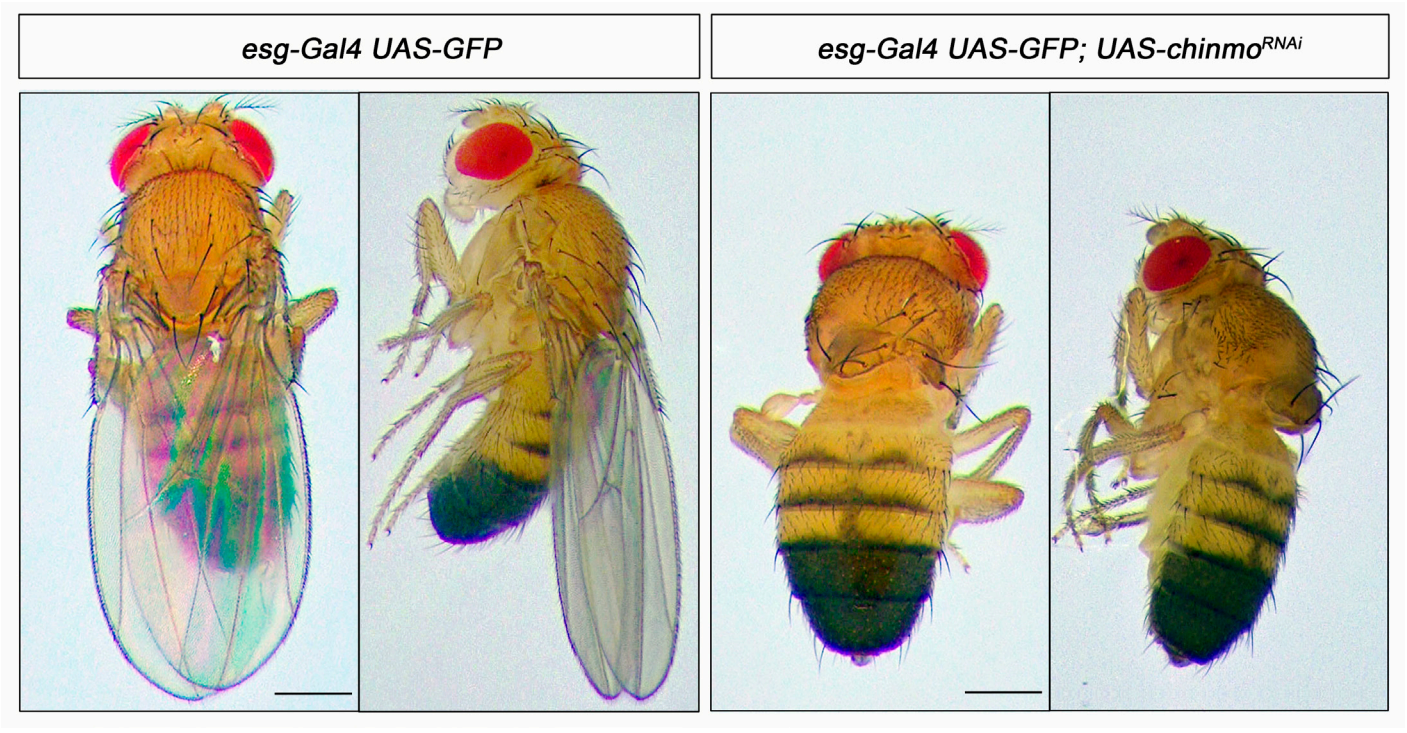

Figure 3—figure supplement 1. Chinmo is required for wing development during the larval period. Dorsal and lateral view of control (right panel) and *UAS-chinmo*^{RNAi} (left panel) adult flies. In the absence of Chinmo, flies emerged without wings. Scale bar represents 1 mm.

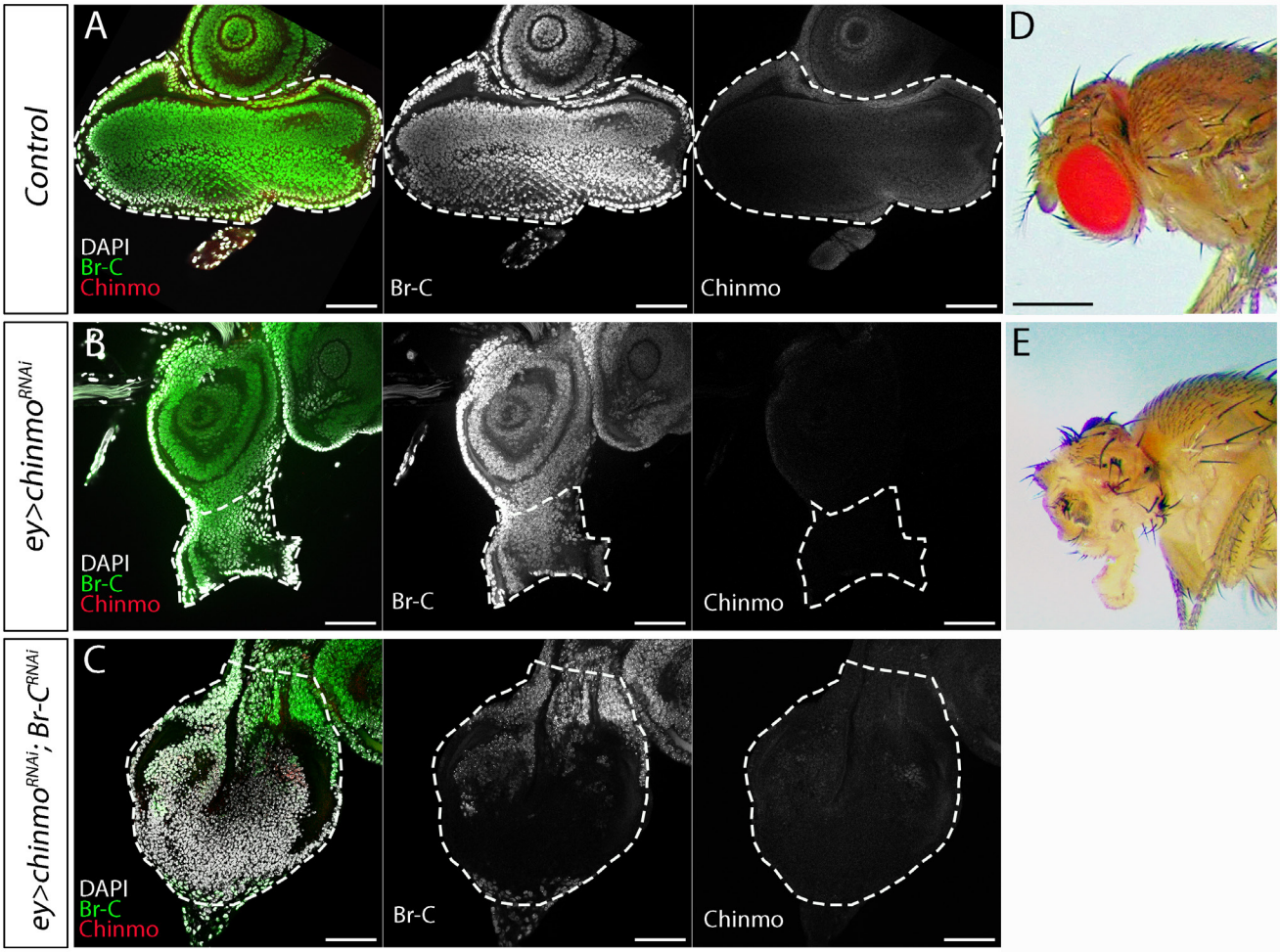

Figure 3—figure supplement 2. *Br-C*-dependent requirement of *chinmo* in the eye disc. (**A–C**) Chinmo (in red), Br-C (in green), and DAPI (in grey) staining in eye discs of control (*ey-Gal4*) (**A**), *UAS-chinmo*^{RNAi} (**B**), and *UAS-Br-C*^{RNAi}*; UAS-chinmo*^{RNAi} (**C**) L3W larvae. The dramatic eye disc reduction induced by the absence of *chinmo* (**B**) was rescued by Br-C depletion (**C**). (**D–E**) Lateral view of control (**D**) and *UAS-chinmo*^{RNAi} (**E**) adult flies. In the absence of Chinmo, flies emerged without eyes. Scale bars represent 50 µm in A–B and 1 mm in D–E. Scale bars represent 50µmin A-C and 1mm in D-E
.

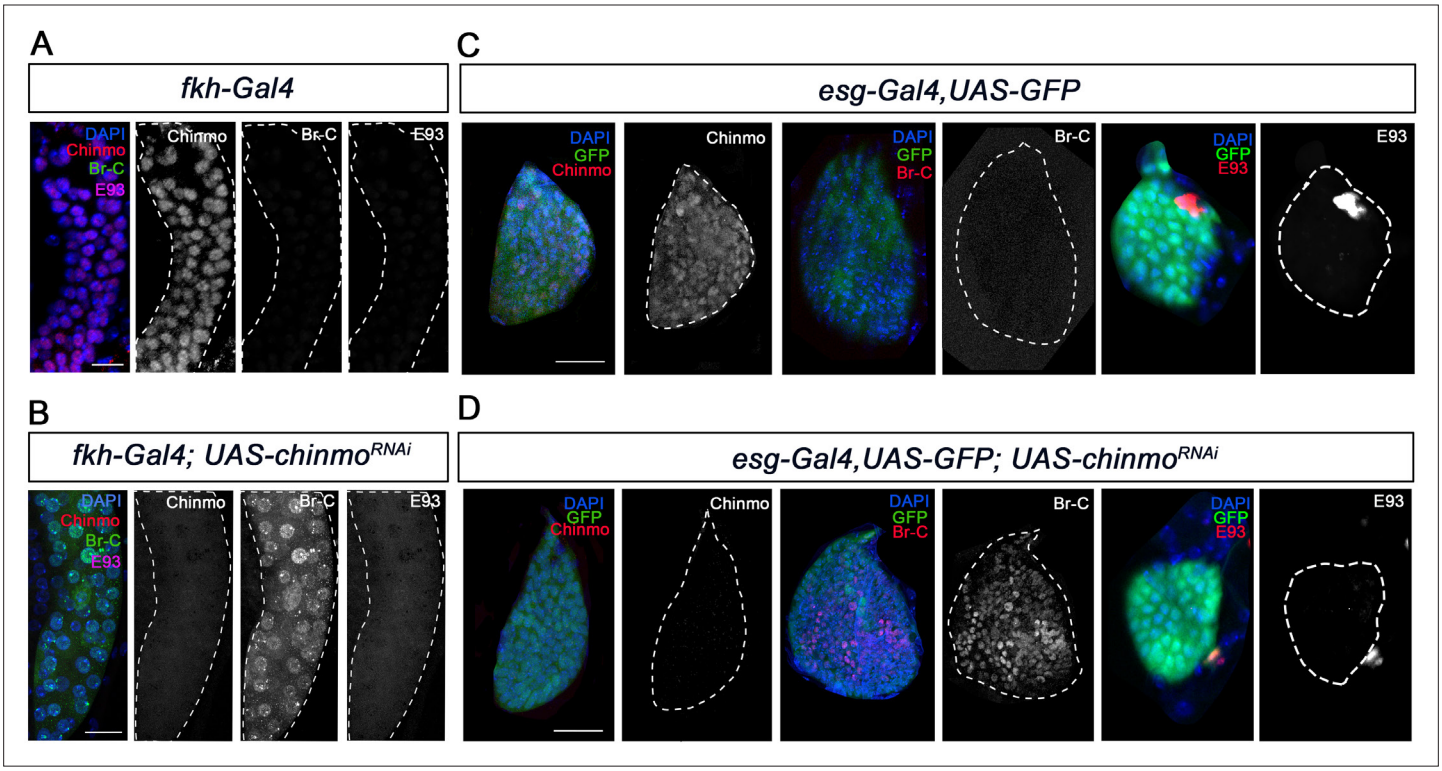

Figure 4. Chinmo represses Br-C in salivary glands and wing discs during early larval development. (**A–B**) Expression of Chinmo, Br-C, and E93 in salivary glands of L1 control (*fkh-Gal4*) (**A**), and *UAS-chinmo*^{RNAi} (**B**). (**C–D**) Expression of Chinmo, Br-C, and E93 in wing discs of early L2 control (*esg-Gal4*) (**C**) and *UAS-chinmo*^{RNAi} (**D**). The *esg* domain is marked with GFP and all cell nucleus with DAPI. In the absence of *chinmo* only *Br-C* shows early upregulation in both tissues. Scale bars represent 25 μm.

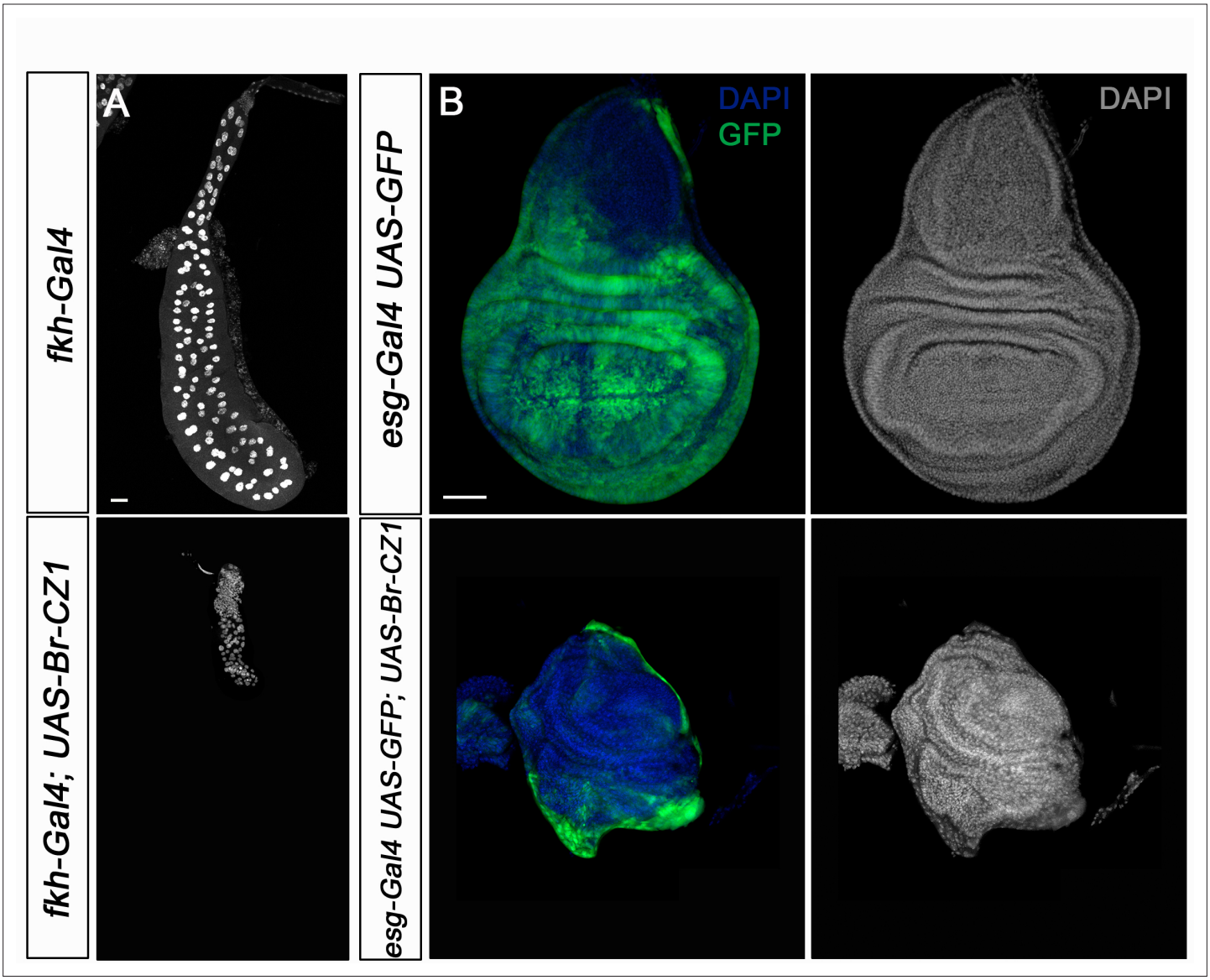

Figure 4—figure supplement 1. Overexpression of Br-CZ1 phenocopies *chinmo* loss of function in SGs and wing discs. (**A**) DAPI-stained SGs from control (*fkh-Gal4*) and *UASBr-CZ1* in L3W larvae. Overexpression of Br-CZ1 impairs SGs grow. (**B**) Wing discs of control (*esg-Gal4*) and *UA-SBr-CZ1* L3W larvae. Wing discs were labelled to visualise the *esg* domain (GFP in green) and nuclei (DAPI). Overexpression of Br-CZ1 in the *esg* domain abolishes wing development. Scale bar represents 50 µm in all panels.

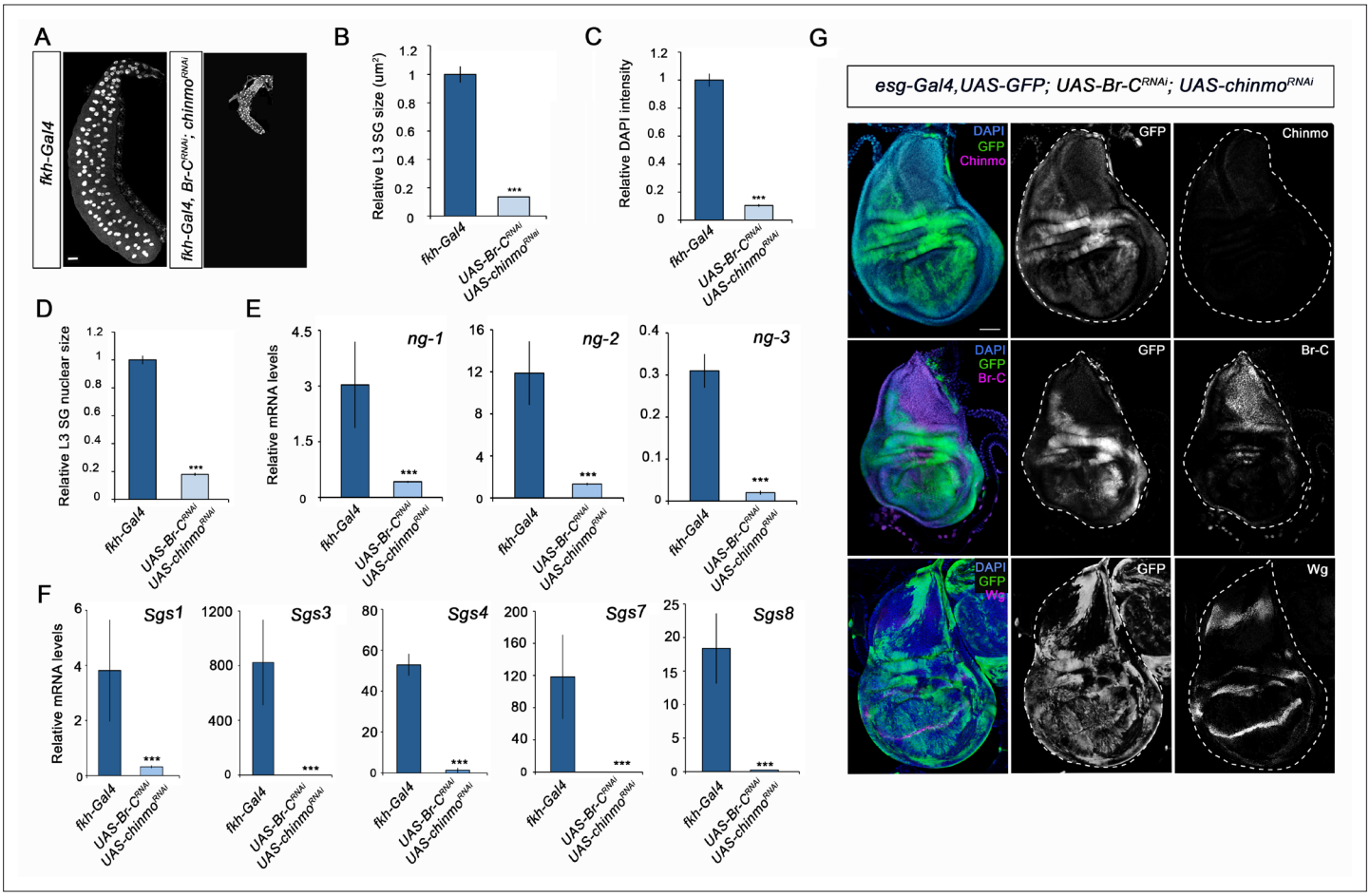

Figure 5. Different requirement of *chinmo* for the larval growth of salivary glands and wing discs. (**A**) DAPI-stained salivary glands from control (*fkh-Gal4*) and *UAS-Br-C^{RNAi}; UAS-chinmo^{RNAi}* L3W larvae. In the absence of *chinmo* and Br-C, salivary glands did not grow. (**B–D**) Comparison of the relative size of salivary glands (n = 10 for each genotype) (**B**), DAPI intensity (n = 50 for each genotype) (**C**), and nucleic size of salivary glands (n = 30 for each genotype) (**D**) of control and *UAS-Br-C^{RNAi}; UAS-chinmo^{RNAi}* L3W larvae. (**E–F**) Relative expression of (**E**) *ng1-3* and (**F**) *Salivary glands secretion* genes in control and *UAS-Br-C^{RNAi}; UAS-chinmo^{RNAi}* L3W larvae measured by quantitative real-time reverse transcriptase polymerase chain reaction (qRT-PCR). Transcript abundance values were normalised against the *Rpl32* transcript. Error bars in B and C indicate the SEM (n = 5–8). Statistical significance was calculated using t test (****p≤0.001). (**G**) Expression of Chinmo, Br-C, and Wg in wing discs of *UAS-Br-C^{RNAi}; UAS-chinmo^{RNAi}* L3W larvae. Wing discs labelled to visualise the *esg* domain (GFP in green). In the absence of *chinmo* and *Br-C*, wing discs grow normally and express Wg correctly. Scale bars represent 50 µm.

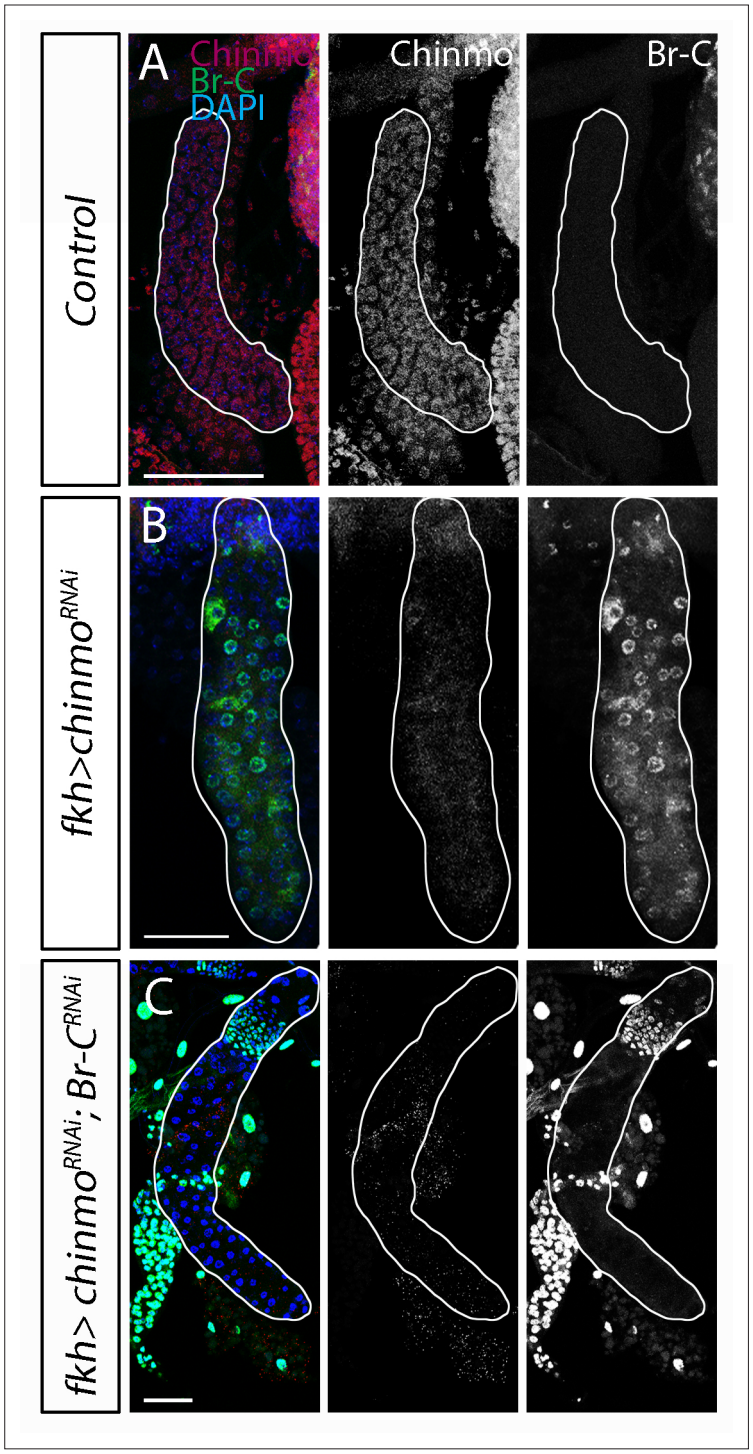

Figure 5—figure supplement 1. Effectiveness of *chinmo* and *Br-C* RNAis in the salivary glands. (**A–C**) Expression of Chinmo (in red) and Br-C (in green) in SG of control (*fkh-Gal4*) (**A**) *UAS-chinmo*^{RNAi} and (**B**) *UAS-Br-C*^{RNAi}*; UAS-chinmo*^{RNAi} (**C**) L2 larvae. Nuclei of SG cells are labelled with DAPI (in blue). Note that the (**C**) double knockdown of *chinmo* and *Br-c* completely abolished the expression of Br-C in the absence of Chinmo (**C**). Scale bars represent 50 µm.

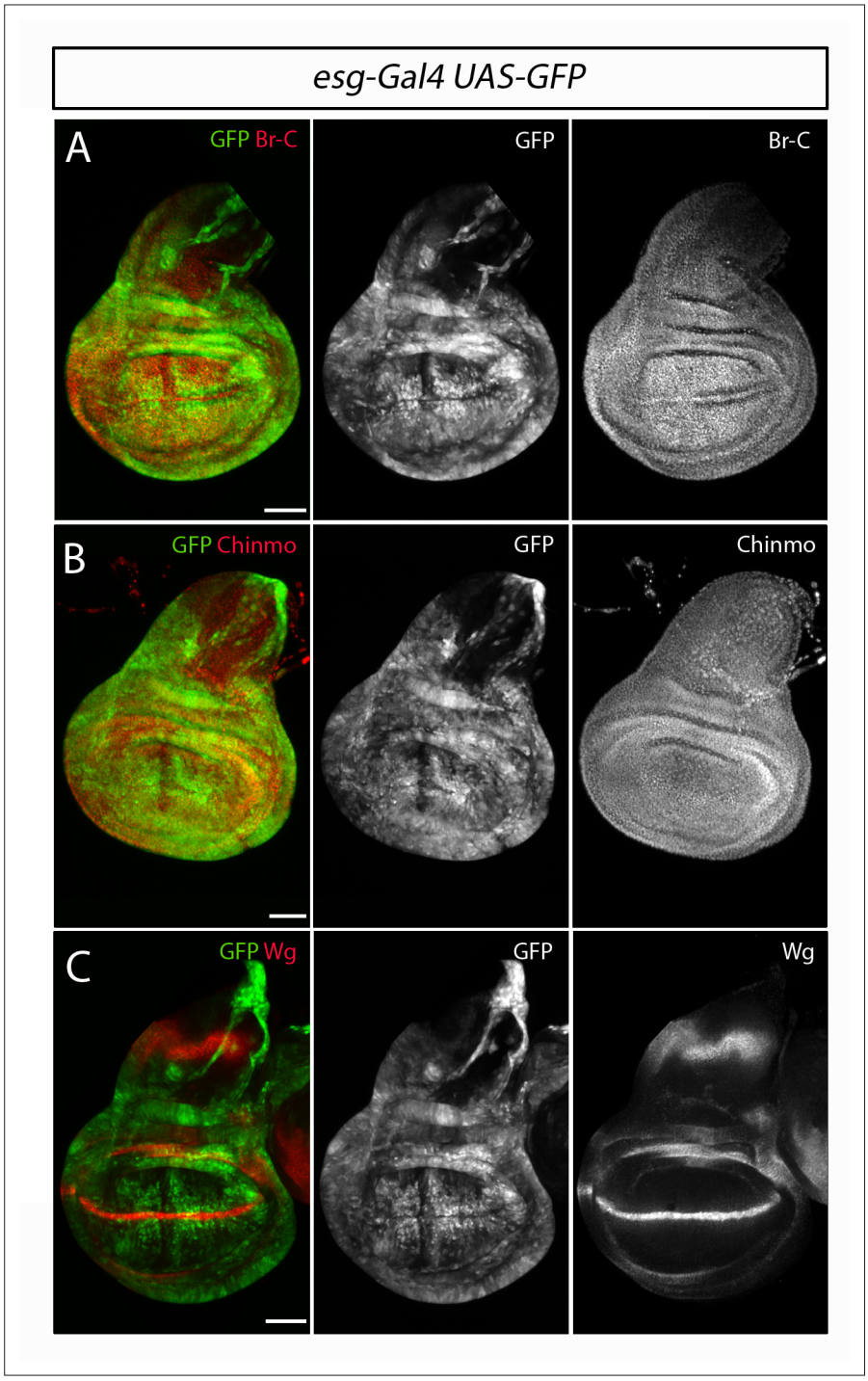

Figure 5—figure supplement 2. Expression of Chinmo and Br-C in the developing wing disc. (**A–C**) Control wing discs, esg-Gal4; UAS-GFP, were labelled to visualise the esg domain in green and in red (**A**) Br-C expression in L3W larvae, (**B**) Chinmo expression in early-mid L3 larvae and (**C**) the morphogenetic marker Wg in L3W larvae. Scale bar represents 50 μm in all panels.

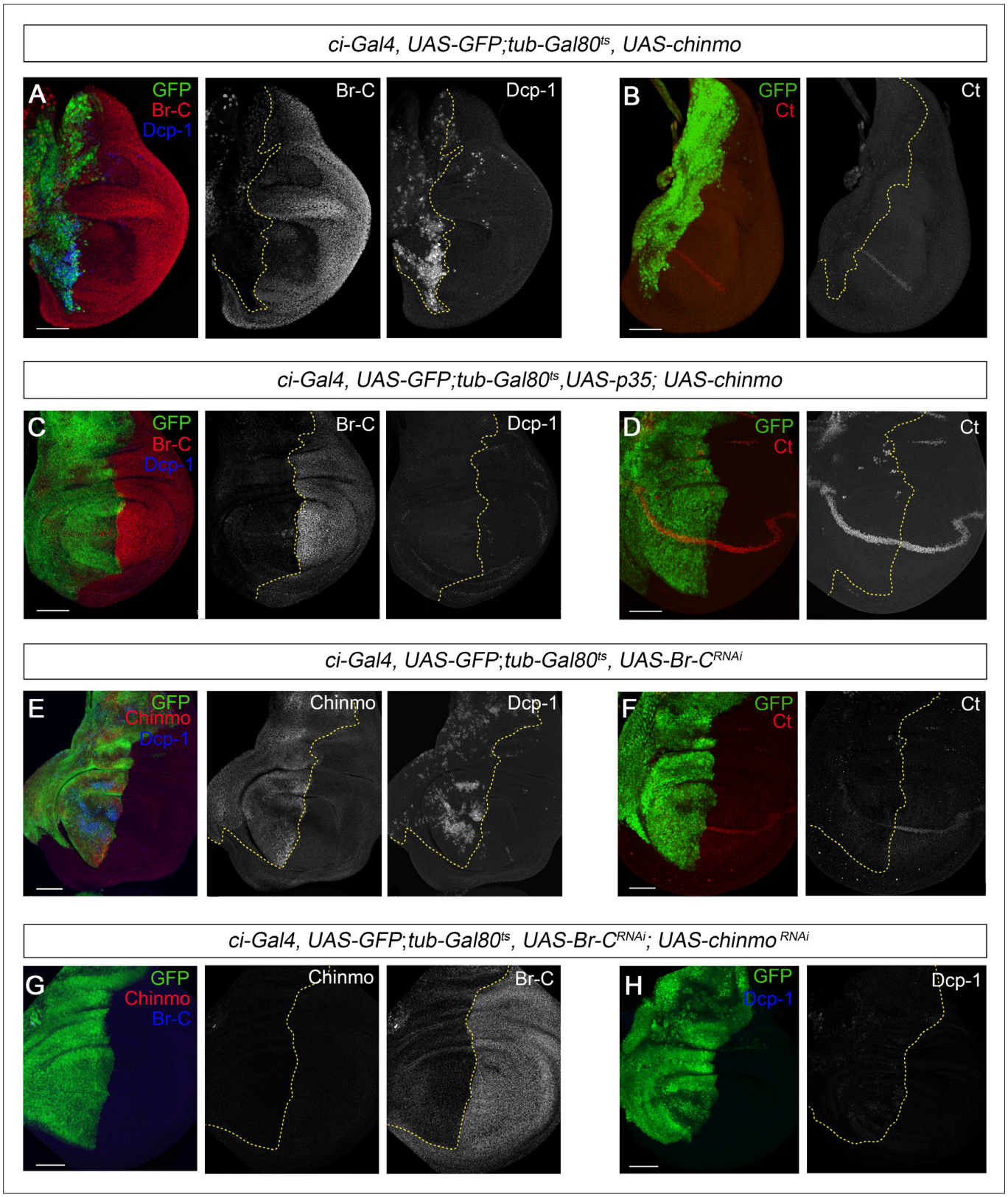

Figure 6. *chinmo* depletion during late L3 is required for proper larva to pupa transition. (**A–H**) Images of wing imaginal discs from L3W larvae. The indicated constructs were expressed under the control of the *ci-Gal4* driver. Overexpression or depletion of the transgenes was activated in early L3 larvae and analyzed at the L3W stage. An *UAS-GFP* construct was used to mark the anterior region of the disc where the transgenes were induced or repressed (green). (**A**) Overexpression of *chinmo* repressed Br-C, induced Dcp-1, and (**B**) abolished Ct. (**C**) Overexpression of *chinmo* together with *p35*

Figure 6 continued on next page

Figure 6 continued

repressed Br-C and blocked Dcp-1, but fails to restore normal expression of Ct (**D**). (**E**) Depletion of *Br-C* induced Chinmo and Dcp-1 and (**F**) repressed Ct. (**G**) In double depletion of *Br-C* and *chinmo* (**H**), Dcp-1 was not detected. Scale bars represent 50 μm.

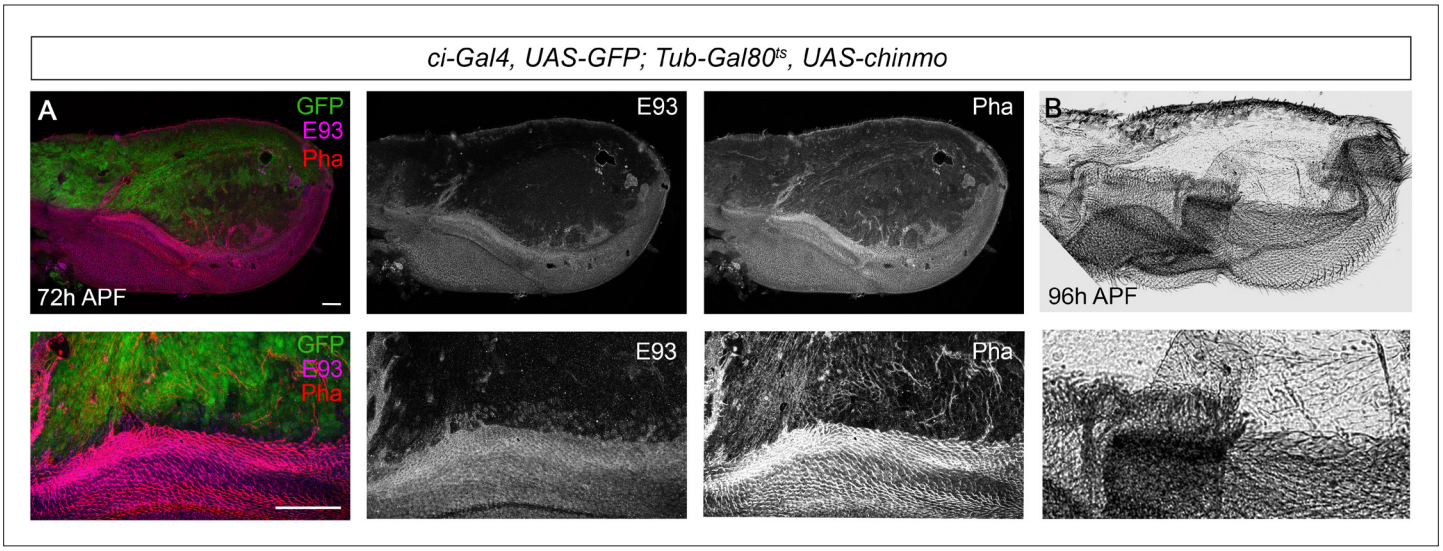

Figure 7. Presence of Chinmo during pupal development blocks adult differentiation. (**A**) Overexpression of *chinmo* in the anterior part of the pupal wing at 72 hr after pupa formation (APF) using *ci-Gal4* driver represses *E93* expression and produced alterations in phalloidin (Pha) pattern. (**B**) Cuticle preparation of a pupal wing at 96 hr APF expressing *chinmo* under the control of the *ci-Gal4* driver. Bottom panels are magnifications from upper images. The scale bars represent 50 μm (top panels) and 100 μm (bottom panels).

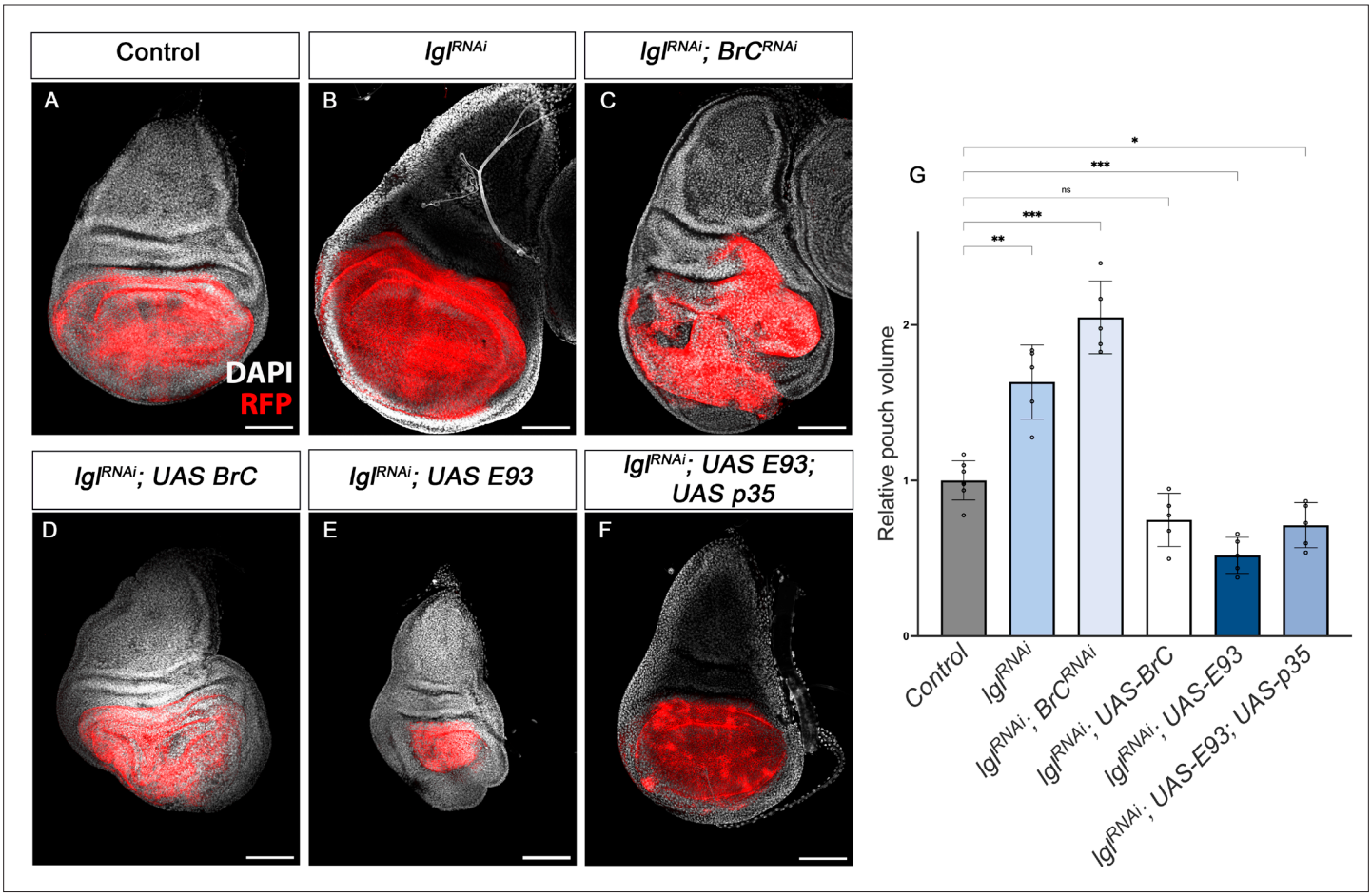

Figure 8. Tumour suppression action of Br-C and E93. (**A–F**) Confocal images of L3 wing imaginal discs. The indicated constructs were expressed under the control of the *nub-Gal4* driver. An *UAS-RFP* construct was used to mark the pouch region of the disc where the transgenes were induced (magenta). Nuclei were labelled with DAPI (grey). Scale bars at 100 μm. (**G**) Volumetric quantification of the RFP-positive area of the wing discs for the indicated groups. The pouch volumes were normalised to the mean of the control. Error bars in G indicate the SEM (n = 10). Welch's ANOVA ($p<0.0001$) followed by Dunnett's T3 post hoc tests (*$p<0.05$, **$p<0.01$, ***$p<0.001$).

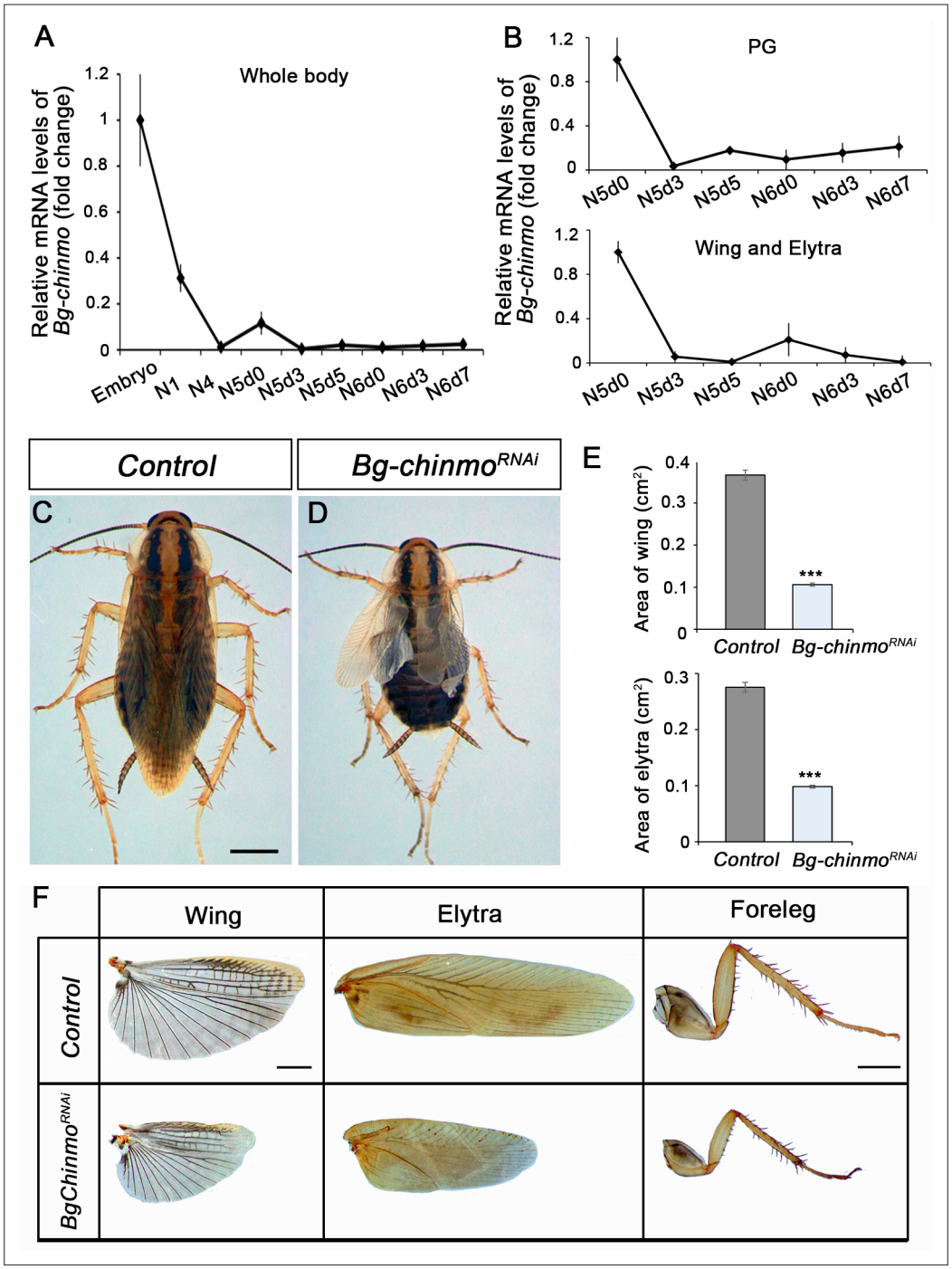

Figure 9. Depletion of *chinmo* in *B. germanica* promotes premature adulthood. (**A–B**) *Bg-chinmo* mRNA levels measured by quantitative real-time reverse transcriptase polymerase chain reaction (qRT-PCR) from embryo to the last nymphal stage (**N6**) in whole body (**A**), and prothoracic gland (PG), and wings and elytra (**B**). Transcript abundance values were normalised against the *Rpl32* transcript. Fold changes were relative to the expression of embryo (for whole body) or N5d0 (for PG and wings and elytra), arbitrarily set to 1. Error bars indicate the SEM (n = 3–5). (**C–D**) Newly moulted N4 nymphs of *B. germanica* were injected with *dsMock* (*Control*) or *dschinmo* (*Bg-chinmo*^{RNAi}) and left until adulthood. (**C**) Dorsal view of adult Control, and (**B**) premature adult *Bg-chinmo*^{RNAi}. (**E**) Quantification of wing and elytra areas (cm^2) of adult Control and *Bg-chinmo*^{RNAi} premature adults. Error bars indicate the SEM (n = 4–6). Statistical significance was calculated using t-test (***p≤0.001). (**F**) Control and *Bg-chinmo*^{RNAi} wing, elytra and foreleg of newly emerged adult of *B. germanica*. The scale bar represents 2 mm.